



Control of the Malt Mashing and Boiling Process in Craft Beer Production: *Hardware-in-The-Loop-Technique*

Steven I. Pogo^(✉), Jhonatan F. Arias, and Víctor H. Andaluz

Universidad de Las Fuerzas Armadas ESPE, Sangolquí, Ecuador
{sipogo, jfarias5, vhandaluz1}@espe.edu.ec

Abstract. This work presents the design of control algorithms based on mathematical models algebra and PID, for the level and temperature control of a craft beer mashing and brewing plant, which will be designed in an immersive and interactive industrial virtual environment in the Unity 3D graphic engine. The controllers are implemented through the Hardware-in-the-Loop technique in order to allow the implementation of advanced control algorithms in an efficient and safe way. The virtual environment considers 3D models that provide a high level of realism to the process and the possibility of interaction with the user, also avoids the risk of damage to the system or loss of real control elements. For the virtualization of the industrial process, the mathematical model of the plant is considered and finally, the experimental results obtained in the implementation of the controllers through the Hardware-in-the-Loop technique are presented by means of a performance analysis of the same within the industrial process.

Keywords: Temperature control · Level control · Hardware-in-the-Loop · Industrial virtual environments · Virtual reality

1 Introduction

Throughout history, the industry has evolved by leaps and bounds [1], making the concept of automation as essential in modern industry in any field of application, since automatic processes play a fundamental role in the manufacture of a wide variety of products that aim to meet the needs of human beings [2], and nowadays, with the growing need to increase production, guarantee product quality and reduce costs, it is increasingly common to implement automatic systems in artisanal processes through classical and advanced control algorithms [3, 4]. For example, in the production of craft beer, fuzzy controllers have been applied in the malt mashing and boiling stages, by means of various actuators depending on the temperature and time of the process [5].

In the mashing process, automatic controls have also been carried out by controlling and monitoring pH, tank levels and temperature, using specific sensors to measure each of the variables and exchanging data with a PC [6]. Within the mashing process, temperature regulation is essential because the activity of enzymes that generate fermentable sugars

depends on this, one of the ways that has been used in the industry to monitor the temperature automatically, for example in [7], is using temperature controllers within a programmable logic controller, as well as in [8], Galileo Intel development and Arduino Mega programming cards have been used, but these cards are not the only ones used to perform this procedure, because in [9] Raspberry Pi cards are also used.

In order to accelerate the algorithm development process for industrial plants, test environments based on the Hardware-in-the-Loop technique have been created [10]. The HIL technique is also used for educational purposes as seen in [11], in order to generate practical experiences eliminating the danger of handling real plants, where the virtual plant controller has been implemented in the same way in embedded cards.

These facts have been the inspiration to propose the implementation of the Hardware-in-the-Loop (HIL) technique for the monitoring and control of craft beer production through an immersive and interactive industrial virtual environment with the user developed in the Unity 3D graphic engine that allows to accelerate the development of control algorithms for real industrial plants and at the same time, that the designed environment allows to be used for educational purposes as it is an interactive environment. For the implementation of the HIL technique, mathematical modeling will be considered to represent the mashing and boiling of malt, with the purpose of implementing advanced control algorithms for the automation of the temperature and level variables of this process.

This document is divided into six sections, including the Introduction. Section 2 presents the development of the virtual environment. Section 3 shows the mathematical modeling of temperature and process level. Section 4 presents the design of the control algorithms. Section 5 shows the results of the implemented virtual system and the developed controllers. Finally, Section 6 presents the conclusions.

2 Virtual Environment

This section presents the industrial process virtualization methodology, which can be divided into four main stages called reference model; 3D modeling; production and integration; and the communication channel, as shown in Fig. 1.

To begin with, a reference model is taken as a starting point in the first stage where characteristics and aspects of a real industrial factory and P&ID diagrams of similar processes are considered, with the objective of making a conceptual design of a mashing and brewing plant for craft beer.

On the other hand, in the 3D modeling process is the design of the MIMO process of mashing and boiling of craft beer, which is developed in Plant 3D software, where the layers are defined for each element (tanks, flanges, pipes, structure, meshes), as well as the dimensions of the design, the structures that contain the tanks to be controlled are also created, the tanks where the mashing and boiling of the wort takes place, the control valves are placed, and the pumps at the outlets of the mashing and boiling tanks, this design has the extension. *dwg*; once the design is finished, the file is exported in a compact binary format that describes the content of the design data in 3D (AutoCAD native format), finally the 3D model is named and saved.

For exporting FBX type formats you take the native file exported from Plant 3D software and then proceed to open the file in 3ds Max software, which helps to get the

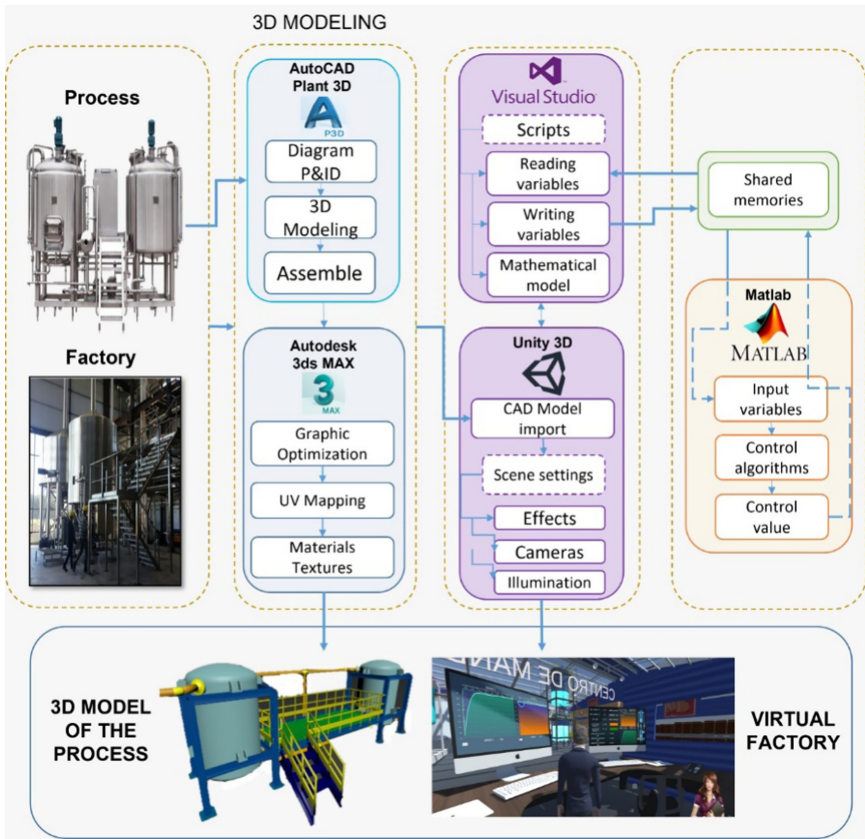


Fig. 1. Industrial plant virtualization methodology

“FBX” file that is recognized by Unity 3D software. Within 3ds Max, once imported, a graphic optimization of the plant is performed by deleting layers and junk figures that are not part of the model, the elements that are part of the layers created in Plant 3D are grouped and assigned a name to make easier its implementation and recognition in Unity, finally an optimization of the textures of the model is performed and the file is saved in FBX format.

Continuing with the virtualization process, you moved on to the stage of integration and production of the 3D virtual environment, in this virtual environment the different characteristics of the process are incorporated, such as heating, liquid filling, exploitations, sounds, textures, among others, making use of the Unity particle system and object-oriented programming in Visual Studio, allowing the virtualized plant to have a greater resemblance to the real plant.

The structure of the bilateral connection between the control board and the Unity software is shown in Fig. 2, which details the three main stages that compose the closed-loop control scheme using the Hardware-in-the-Loop technique, according to [12]. The

first stage frames the target controller, which is constituted by a Raspberry Pi embedded board, which contains the control algorithm for both level and temperature, based on mathematical model algebra and PID. The second stage consists of the real time simulation of the process, implemented in the graphic software Unity 3D, where the behavior of the mashing and cooking plant is simulated. The modeling of the level and temperature process is immersed in the Visual Studio programming software, receiving the control commands for the final control elements, as well as allowing the addition of perturbations to the system. Finally, the third stage refers to the communication channel, which in this case will be wireless, this will be in charge of communicating the real part of the process with the simulation block in real time.

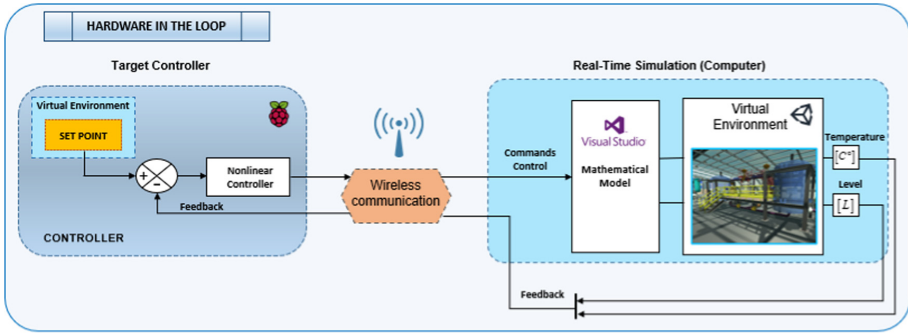


Fig. 2. Hardware-in-the-Loop based control structure.

3 Process Modeling

3.1 Level Model

The leveling process is shown in Fig. 3, consisting of two tanks (Tk1, Tk2), a pump to provide a constant flow for fluid exchange between the tanks, five control valves $a \in R[0 - 1]$ distributed in three adjustable valves (a_1, a_2, a_3) to control the inlet flow of each tank, two solenoid valves ON/OFF (a_4, a_5) that allow one-way flow in the fluid exchange, and a loading valve that allows the fluid to flow in one direction only (a_0) for the system output will also be used to cause disturbances in the stability analysis of the controller.

A continuous and constant inflow is assumed, while the Torricelli theorem is used for the outflow from the tanks, which relates the fluid velocity to the cross-sectional area and its flow is limited by the solenoids valve (EV: a_4, a_5)

$$q_4 = a_4 S_1 \sqrt{2gh_1(t)} \quad (1)$$

$$q_3 = a_3 S_2 \sqrt{2gh_2(t)} \quad (2)$$

where g : gravitational constant; S_1 and S_2 : cross-sectional area of each outlet pipe (tanks one and two); h_1 and h_2 : height of tanks one and two, respectively.

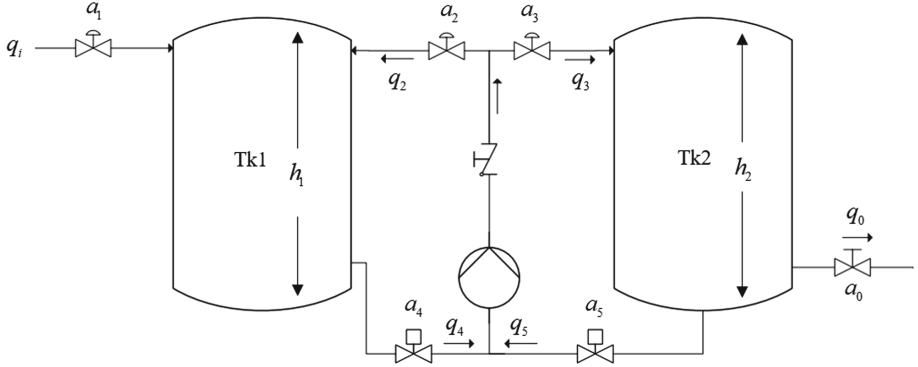


Fig. 3. Maceration and cooking process

For the dynamics of fluids between tanks, the application of the theory of the quantity of motion to a momentum theory as presented in [13]. Where the output velocity of the driving mechanism is equal to the sum of the input velocities (v_i) and output of the driving propeller (v_e), expressed in (3).

$$v_b = \frac{1}{2}(v_i + v_e) \quad (3)$$

Multiplying this equality by the cross-sectional area of the pipes gives the pump output flow, this flow is equal to the tank output flow plus the flow provided by the pump.

$$q_b = \frac{1}{2}(q_4 + q_5 + K_1 V_1) \quad (4)$$

where $K_1 V_1$: is the pump flow rate which depends on the pump constant K_1 and the voltage supplied to the pump V_1 .

The volume variation (m^3) of each tank is affected by the liquid entering and leaving the tank, where the area of the tank bottom is constant (m^2) therefore, the head (m) varies with time depending on the flow rate into and out of the tank.

$$A_1 \frac{dh_1}{dt} = a_1(t)q_i + a_2(t)q_b - a_3(t)q_b \quad (5)$$

$$A_2 \frac{dh_2}{dt} = a_3(t)q_b - a_2(t)q_b - a_0(t)S_3 \sqrt{2gh_2(t)} \quad (6)$$

where A_1 and A_2 : cross-sectional area of each tank (tanks one and two); the flow and outlet flows are regulated by the control valves, while the process outlet flow is regulated by the loading valve $a_0(t)$.

The mathematical model in Fig. 2 is expressed in the form of a matrix, with the corresponding values of the control valve openings as well as the load valve a_0 denominated with the letter L:

$$\begin{bmatrix} \dot{h}_1(t) \\ \dot{h}_2(t) \end{bmatrix} = \begin{bmatrix} \frac{q_i}{A_1} & \frac{q_b}{A_1} & -\frac{q_b}{A_1} \\ 0 & -\frac{q_b}{A_2} & \frac{q_b}{A_2} \end{bmatrix} \begin{bmatrix} \dot{a}_1(t) \\ \dot{a}_2(t) \\ \dot{a}_3(t) \end{bmatrix} + \begin{bmatrix} 0 \\ -\frac{s_3 \sqrt{2gh_2}}{A_2} \end{bmatrix} [a_0]$$

$$\dot{\mathbf{h}}(t) = \mathbf{A}\mathbf{u}(t) + \boldsymbol{\eta} \quad (7)$$

where, q_i : input flow; q_o : outward flow; $\mathbf{h} \in \mathbb{R}^{2 \times 1}$: corresponding to the coefficients of the variations of the heights; $\mathbf{u} \in \mathbb{R}^{3 \times 1}$: corresponding to the coefficients of the valve openings; $\boldsymbol{\eta} \in \mathbb{R}^{2 \times 1}$: corresponding to the load matrix of the outlet valve. La Fig. 4 shows the validation of the performance of the mathematical model (7) for the level process in the mashing and boiling of malt.

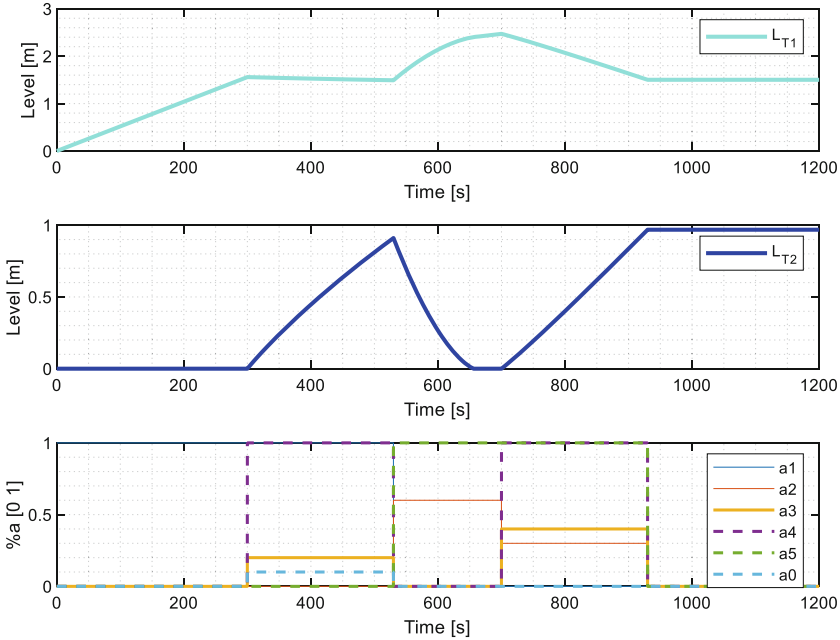


Fig. 4. Level model validation

The tanks start with initial conditions of 0 [m] for each one, from the first second until 300 [s] the valve a_1 is completely open and the others are closed, which fills only Tk1; from 300 [s] to 530 [s] the EV a_4 is enabled for fluid transfer between Tk1 and Tk2 with an opening percentage of 20% for the valve a_3 whereby Tk2 starts to receive fluid from Tk1, from 530 [s] to 700 [s], the valve closes a_1 , the EV a_4 and the valve is enabled a_5 with an opening percentage of 60%, this completely empties Tk2 and sends all the liquid to Tk1, then the two EV are enabled and an opening percentage of 30% is given for a_2 and 40% for a_3 , for a fluid exchange to take place between the two tanks and the final valve was closed, so the level reached up to that moment is maintained.

3.2 Temperature Model

Steam is an essential part for the different stages of the brewing process and mainly to heat the water where the malt and hops will be dissolved [14]. It is also efficient at

transferring heat through condensation, so a shell and tube heat exchanger are used as shown in Fig. 5, to heat the liquid inside the tank and take advantage of the liquid flow to recirculate while heating.

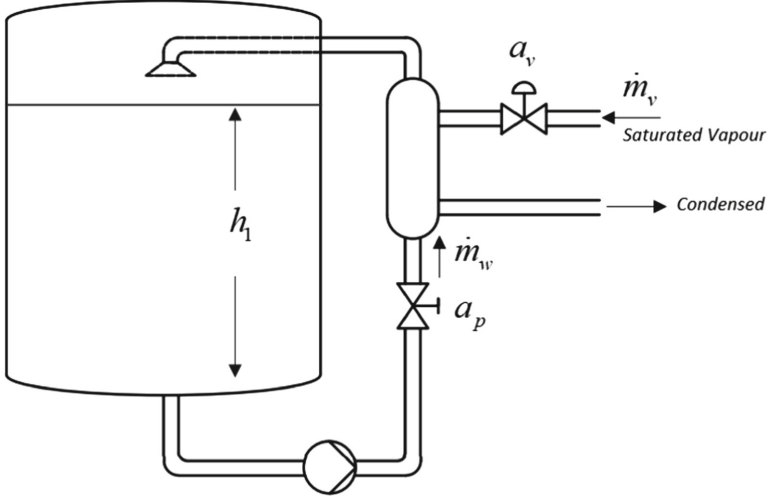


Fig. 5. Heating process with shell and tube heat exchanger

In Fig. 5 the mass flow is defined as \dot{m}_v and as \dot{m}_w for the liquid inlet, in the case of the vapor mass flow it depends on the dynamics of the vapor control valve a_v .

$$\dot{m}_v = a_v(t)K_v\sqrt{\Delta P} \quad (8)$$

in the case of the mass flow of the liquid depends on the flow of the pump that drives the liquid to the exchanger, this flow is regulated by a load valve a_p .

$$\dot{m}_w = a_p(t)K_2V_2 \quad (9)$$

where a_v y $a_p \in R[0 - 1]$; K_v : valve constant; ΔP : upstream and downstream pressure variation; K_2 : pump constant, V_2 : voltage supplied to the pump.

The energy balance on the element to which heat is transferred is given by the heat capacity ratio of the fluids involved in the heat exchanger multiplied by the temperature change of that fluid.

$$\dot{Q}_i = \dot{m}C_p(T_i - T_o) \quad (10)$$

where T_i : inlet temperature of the fluid and T_o : outlet temperature, to this is added the heat transferred from the surface through which the hot and cold fluid circulates, the heat transfer rate in a heat exchanger can be expressed by Newton's cooling law [14].

$$\dot{Q}_t = UA_s(T_h - T_c) \quad (11)$$

where U : Convection transfer coefficient; A_s : surface area where the fluids circulate; T_h : Temperature of the hot fluid; T_c : Temperature of the cold fluid; he stored instantaneous energy can be defined as the input energy (Q_i) plus the transferred energy (Q_t). Therefore, the energy balance can be established as follows

$$mC_p \frac{dT}{dt} = Q_i + Q_t \tag{12}$$

Finally, the energy balance equation is defined as follows:

$$m_p C_{pw} \frac{T_0}{dt} = \dot{m}_w C_{pw} (T_i(t) - T_o(t)) + UA_s (T_v(t) - T_o(t)) \tag{13}$$

$$m_v C_{pv} \frac{T_v}{dt} = \dot{m}_v h_{fg} - UA_s (T_v(t) - T_o(t)) \tag{14}$$

where m_p : is the mass of the process contents; T_o : outlet temperature of the heat exchanger; T_i : inlet temperature; T_v : vapor temperature; h_{fg} : vaporization enthalpy; the mass of the process can be expressed as the product of the volume contained in the tank by the density ($m_p = \rho V_{Tk}$), which can be related to the level of the tanks described in (7).

The calculation of the convective transmission coefficient is obtained experimentally and depends on the flow rate of the fluids, the calculation of U is based on [15] and [16] where the analysis is performed for a single-pass heat exchanger, however, the process can be used for multi-pass heat exchangers. A schematic diagram of the heat exchanger is shown in Fig. 6 where the saturated steam enters the shell \dot{m}_v and upon heat transfer by condensation leaves the shell as a liquid due to gravity, while the cold liquid \dot{m}_w passes through the tubes and receives the heat transferred through the pipe walls with an inner radius and an outer radius r_o .

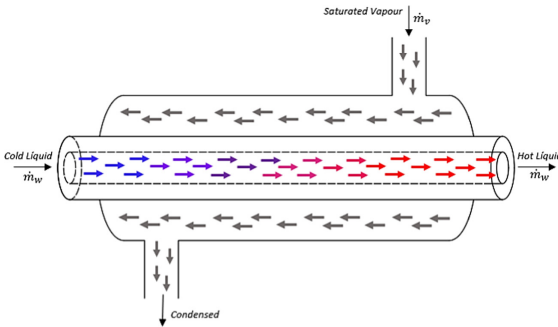


Fig. 6. Shell and tube exchanger Schematic

The area of the heat transfer section is given by:

$$A_s = 2\pi r_o L_t \tag{15}$$

where, L_t is the length of the pipe where the liquid flow circulates.

The general convection heat transfer coefficient U is calculated dynamically using the mechanical conditions of the hot and cold fluids as they enter the heat exchanger, it is important to consider the heat transfer coefficient of the tube H_t and the shell H_s , the convection coefficient for each fluid is calculated by:

$$H = \frac{N_u}{kD_h} \quad (16)$$

where k : is the thermal conductivity of the fluid and its value depends on the temperature of each fluid; D_h : Hydraulic diameter; N_u : Nussel number; it is important that the convective heat transfer coefficient (U) includes the heat conduction coefficient H_c by means of the pipe thickness: $b_t = r_0 - r_i$; and the conductivity coefficient of the pipe material and is calculated as follows:

$$H_c = \frac{k_t}{b_t} \quad (17)$$

Therefore, the overall heat transfer coefficient is determined as follows

$$U = \left(\frac{1}{H_t} + \frac{1}{H_s} + \frac{1}{H_c} \right)^{-1} \quad (18)$$

The Fig. 7 shows the validation of the performance of the mathematical model (13) and (14) for the temperature process in malt cooking and mashing.

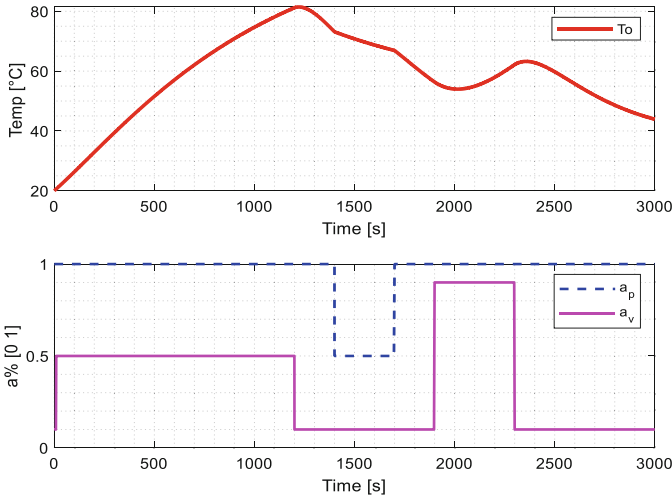


Fig. 7. Temperature model validation

The outlet temperature of the exchanger starts with initial conditions of 20° which is the ambient temperature and the vapor valve a_v is at 50% opening and reaches a temperature of 80°C , from 1200 [s] the valve is closed by 10% which causes a temperature drop, while the temperature decreases in the range of 1400 [s] to 1700 [s] the disturbance valve a_p closes by 50% which causes the liquid flow is lower so that the temperature begins to decrease with less speed.

4 Controller Design

In this section, the design of a level control algorithm based on mathematical model algebra is presented; on the other hand, PID algorithms are implemented for temperature control. Finally, the performance of the control algorithms in the level and temperature process is analyzed.

4.1 Controller Based on Inverse Behavior of the Process.

The method to be developed using the inverse plant behavior is illustrated in Fig. 8, the plant behavior is obtained from (7).

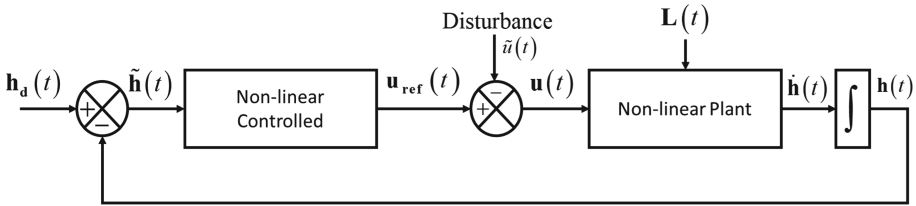


Fig. 8. Control algorithm based on the inverse behavior of the plant

where \mathbf{h}_d : is the vector of desired head; \mathbf{h} : is the vector of the process head; $\tilde{\mathbf{h}}$: is the vector of error ($\mathbf{h}_d - \mathbf{h}$); $\boldsymbol{\eta}$: is the vector representing the system load; \mathbf{u} : is the vector of the process inputs (valve opening); \mathbf{u}_{ref} : is the vector containing the process control actions, defined as

$$\mathbf{u}_{\text{ref}}(t) = \mathbf{A}^{-1}(\mathbf{K}\tilde{\mathbf{h}}(t) - \boldsymbol{\eta}(t)) \quad (19)$$

where \mathbf{A}^{-1} : is the inverse of the plant behavior; $\mathbf{K} \in R^{2 \times 2}$ is a fit matrix.

Stability and Robustness Analysis. The behavior of the error $\tilde{\mathbf{h}}$ in the level process for the mashing and boiling of malt is analyzed considering perturbations at the plant input defined as

$$\tilde{\mathbf{u}}(t) = \mathbf{u}_{\text{ref}}(t) - \mathbf{u}(t) \quad (20)$$

The disturbances at the plant input may be due to the noise generated in the communication between the controller and the final control element.

Considering (20), (19) and (7) the closed loop equation is determined as follows

$$\dot{\tilde{\mathbf{h}}} = -\mathbf{K}\tilde{\mathbf{h}} + \mathbf{A}\tilde{\mathbf{u}} \quad (21)$$

According to [17], for the stability and robustness analysis, the Lyapunov candidate function $\mathbf{V}(\tilde{\mathbf{h}}) = \frac{1}{2}\tilde{\mathbf{h}}^T\tilde{\mathbf{h}}$, is considered, it is derived as a function of time to determine the evolution of the errors $\dot{\mathbf{V}}(\tilde{\mathbf{h}}) = \tilde{\mathbf{h}}^T\dot{\tilde{\mathbf{h}}}$ therefore, when replacing in (21) we obtain

$$\dot{\mathbf{V}}(\tilde{\mathbf{h}}) = -\tilde{\mathbf{h}}^T\mathbf{K}\tilde{\mathbf{h}} + \tilde{\mathbf{h}}^T\mathbf{A}\tilde{\mathbf{u}} \quad (22)$$

for (22) to be negative definite it must be satisfied that $\dot{\mathbf{V}}(\tilde{\mathbf{h}}) < 0$, therefore

$$\|\mathbf{K}\tilde{\mathbf{h}}\| > \|\mathbf{A}\tilde{\mathbf{u}}\| \quad (23)$$

when the condition of (23) is fulfilled, the error $\tilde{\mathbf{h}}$ is considered to be bounded by

$$\|\tilde{\mathbf{h}}\| < \frac{\|\mathbf{A}\tilde{\mathbf{u}}\|}{\lambda_{\min}\mathbf{K}} \quad (24)$$

it can be concluded that, when there are disturbances at the input of the plant ($\tilde{\mathbf{u}}$) the error $\tilde{\mathbf{h}}$ is bounded by (24) and the system is stable, where λ_{\min} : are the minimum eigenvalues; are the minimum eigenvalues ($\tilde{\mathbf{u}} = 0$) the control error $\tilde{\mathbf{h}}(t) = \mathbf{0}$ when $t \rightarrow \infty$, so it is an asymptotically stable system.

4.2 PID Controller

The PID Control is a control strategy that combines proportional, integral and derivative actions, with the objective of correcting the error between the measured value and the desired value or Set Point. The general equation of the PID controller is as follows:

$$u(t) = K_p e(t) + \frac{K_p}{T_i} \int_0^t e(t) dt + K_p T_d \frac{de(t)}{dt} \quad (25)$$

where u and e are the control signal and the control error respectively. The control signal is given by the sum of the proportional term P , integral I and the derivative term D . The tuning parameters of the controller are: the proportional gain K_p , T_i is the integral time and T_d is the derivative time.

5 Experimental Results

This section presents the implementation of the HIL technique for the mashing and boiling process in the brewing process of Fig. 2, where the mathematical model of level and temperature together with the virtual environment is located in the main computer that is characterized by having a Windows 10 operating system, 16 GB of Ram memory, Intel Core i7 processor of tenth generation and 6 GB video card, while the control algorithms are located in the Raspberry PI-4 card, while the bilateral communication between the process and the controller is done through the Xbee wireless modules. The implementation of the Hardware-in-the-Loop technique is shown in Fig. 9.

The Fig. 10 shows the interactive environment with the user, which consists of a control center in the virtual environment, by means of which the process can be controlled through the computer peripherals and the evolution of the variables can be visualized on an HMI interface.

In the development of the virtual environment different features are placed to give greater realism to the implemented process, this is achieved through explosions, irrigation of the liquid in the tanks, movement of the valves, as shown in Fig. 11.

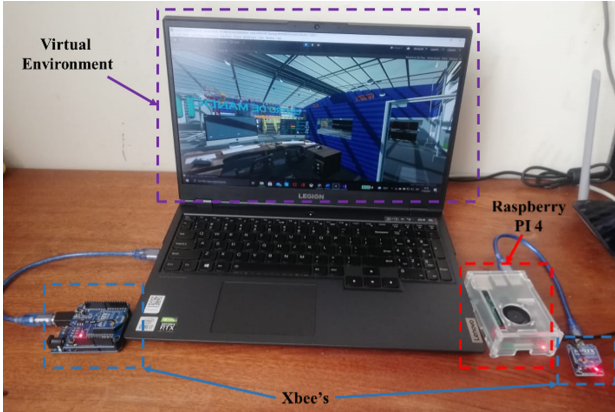


Fig. 9. HIL implementation of mashing and cooking process.



Fig. 10. Command center in the virtual environment.

5.1 Controller Based on Inverse Behavior of the Process

The Fig. 12 shows the performance of the control algorithm based on the inverse behavior of the plant (19), where the behavior of the plant with different values in the desired height vector was evaluated.

From 500 [s] a desired height $h_{d1} = 0.95[m]$ and $h_{d2} = 0.7[m]$ was entered because the desired value change increases from the previous value for both tanks, the algorithm first fills the T_{k2} up to the desired height once the point is reached proceeds to fill the T_{k1} . To perform a stability analysis of the controller, the load valve a_0 was opened with different values during the process, where the controller compensated the disturbance generated by the load, as a result it is concluded that the control algorithm is uniformly asymptotically stable and for disturbances at the input of the plant ($\tilde{\mathbf{u}}$) greater than 10% in the vector of control actions (\mathbf{u}_{ref}) becomes unstable.

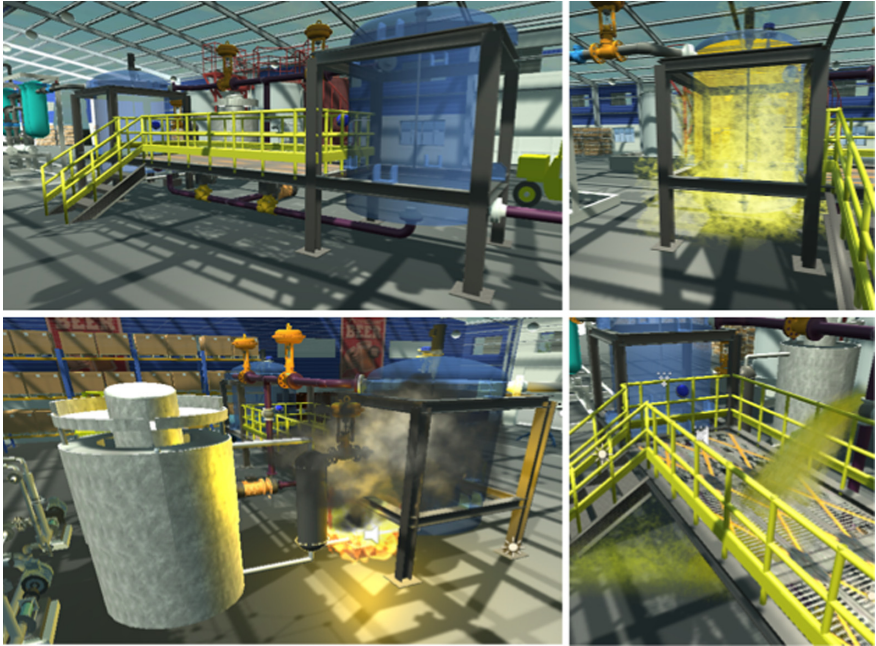


Fig. 11. Realism effects in the process.

5.2 Control PID

In the Fig. 14 shows the performance of the PID control algorithm tuned with the Ziegler-Nichols method and the limiting gain (Fig. 13).

The process starts with the ambient temperature of 20 °C and a temperature scan is performed, as is common in the process terms the temperature evolution is slow with a percentage of over impulse and steady state error of 1 °C, The Fig. 15 shows the control actions sent by the PID from 950 [s] to 1250 [s] the cold flow load valve is varied, which causes the oscillations to extend for a while until returning to the equilibrium point, which determines the stability of the controller.

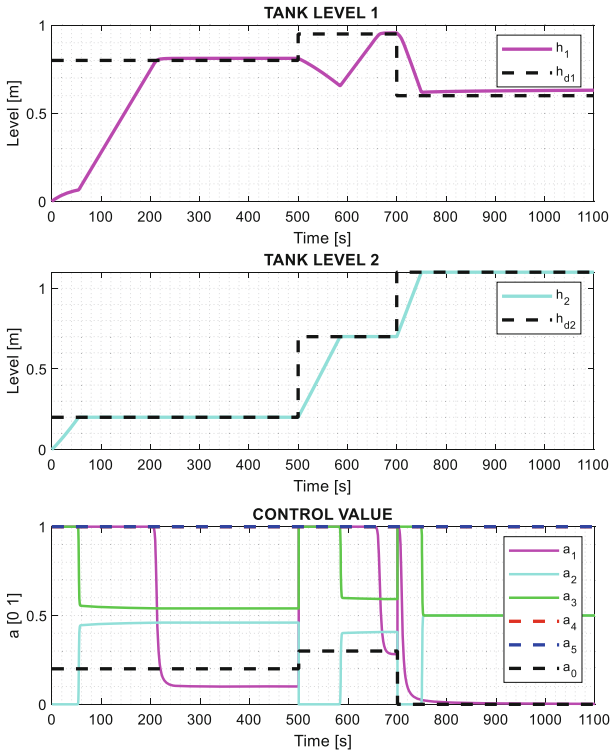


Fig. 12. Performance level control algorithm

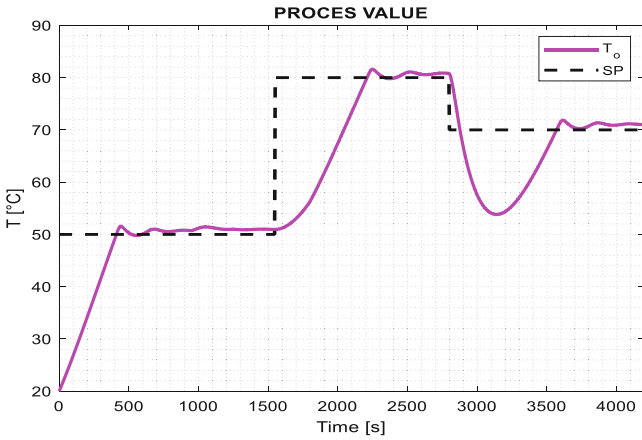


Fig. 13. Performance of the temperature control algorithm

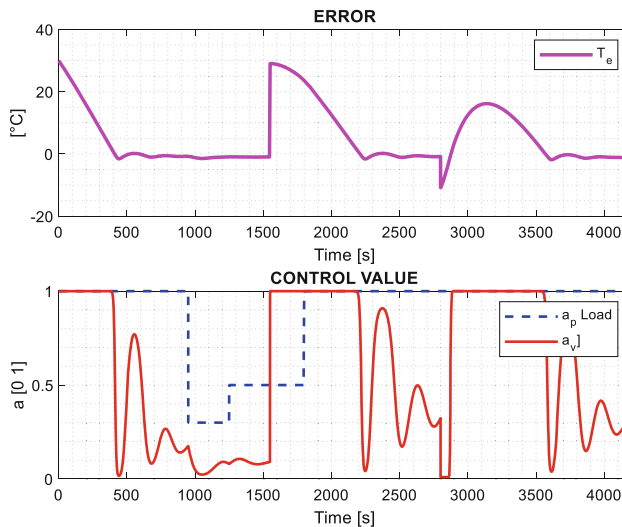


Fig. 14. Evolution of PID controller for the temperature process.

6 Conclusions

Hardware-in-the-Loop is an alternative simulation technique that allows the implementation of advanced control algorithms in processes that present disadvantages due to their high cost or availability. The HIL technique allows to evaluate in real time the behavior of the industrial process, for which it is important to obtain a mathematical model that adequately represents the behavior of the process. The automation of artisanal processes through the application of advanced controllers makes it possible to obtain greater productivity and improve the quality of raw material processing, as in the case of malt mashing and boiling, which requires a scaled temperature control for brewing beer, in addition to achieving product standardization and reducing production costs by significantly reducing raw material losses during the process.

Acknowledgment. The authors would like to thank the Universidad de las Fuerzas Armadas ESPE and the ARSI Research Group for their support in the development of this work.

References

1. Rozo-García, F.: Revisión de las tecnologías presentes en la industria 4.0. *Rev. UIS Ing.* **19**, 177–191 (2020). <https://doi.org/10.18273/revuin.v19n2-2020019>
2. González-Filgueira, G., Javier, F., Permy, R.: Automatización de una planta industrial de alimentación mediante control distribuido. *RISTI Rev. Ibérica Sist. e Tecnol. Informação* (27), 1–17 (2018). <https://doi.org/10.17013/risti.27.1-17>, ISSN-e 1696–9895
3. Nieto, E.C.: Manufactura y automatización Manufacturing and automation. *Ing. Investig* **26**(3), 120–128 (2006). ISSN 0120–5609

4. Oviedo, I.D., Altamirano, C.A., Millan, M.E., Arreaga, N.X., Padilla, V.S.: Development of a prototype of an automatic system for shrimp farming using telecontrol as a viable proposal for small producers. In: Proceedings - 2017 European Conference on Electrical Engineering and Computer Science, EECS 2017, pp. 477–483. Institute of Electrical and Electronics Engineers Inc. (2018). <https://doi.org/10.1109/EECS.2017.94>
5. Perafan, R.M., Meneses, F.C.G., Guerrero, N.P., Saavedra, J.E., Torres, D.M.: Design of a mechatronic prototype to control the milk coagulation process in cheese making. In: 2020 9th International Congress of Mechatronics Engineering and Automation, CIIMA 2020 - Conference Proceedings. Institute of Electrical and Electronics Engineers Inc. (2020). <https://doi.org/10.1109/CIIMA50553.2020.9290323>
6. Luján Corro, M., Vásquez Villalobos, V.: Automatic control with fuzzy logic of home-made beer production in maceration and cooking stages. *Sci. Agropecu.* **1**, 125–137 (2010). <https://doi.org/10.17268/sci.agropecu.2010.02.03>
7. Benitez Baltazar, V.H., Morales Rivas, C.O.: Automatización del proceso de macerado de la malta para la producción de cerveza artesanal. *Epistemus* **12**, 53–61 (2018). <https://doi.org/10.36790/epistemus.v12i24.68>
8. Rodriguez, L., Vinces, L., Mata, N., Del Carpio, C.: Development of an Automatic Equipment for Craft Beer Maceration. In: 2019 Congreso Internacional de Innovación y Tendencias en Ingeniería, CONIITI 2019 - Conference Proceedings. Institute of Electrical and Electronics Engineers Inc. (2019). <https://doi.org/10.1109/CONIITI48476.2019.8960840>
9. Profesional, U., et al.: Instituto Politécnico Nacional, Escuela Superior de Ingeniería Mecánica y Eléctrica (2017)
10. Joaquín Castillo Salinas, D., Pavesi, L.: Proyecto de automatización de planta de cerveza artesanal Easy Brewing. Universidad Andrés Bello (2017)
11. Jorque, B.S., Mollocana, J.D., Ortiz, J.S., Andaluz, V.H.: Mobile manipulator robot control through virtual hardware in the loop. In: Rocha, Á., Adeli, H., Dzemyda, G., Moreira, F., Ramalho Correia, A.M. (eds.) *WorldCIST 2021. AISC*, vol. 1365, pp. 80–91. Springer, Cham (2021). https://doi.org/10.1007/978-3-030-72657-7_8
12. Ortiz, J.S., Palacios-Navarro, G., Andaluz y, V.H., Guevara, B.S.: Marco basado en la realidad virtual para simular algoritmos de control para tareas de asistencia robótica y rehabilitación a través de una silla de ruedas de pie. *Sensores* **21**(15), 5083–5092 (2021)
13. Streeter, V.L.: *Mecánica de los fluidos*. Mc Graw-Hill, DF. Mexico (1970)
14. Más información sobre el vapor | Spirax Sarco. <https://www.spiraxsarco.com/learn-about-steam>, Accessed 11 Aug 2021
15. Çengel, Y.A.: *Transferencia de calor y masa un enfoque practico*. McGraw-Hill, México, D.F. (2007)
16. Bastida, H., Ugalde-Loo, C.E., Abeysekera, M., Xu, X., Qadrdan, M.: Dynamic modelling and control of counter-flow heat exchangers for heating and cooling systems. In: 2019 54th International University Power Engineering Conference UPEC 2019 – Proceedings, pp. 1–6 (2019). <https://doi.org/10.1109/UPEC.2019.8893634>
17. Bonilla, E., Rodriguez, J., Acosta y, J., Andaluz, V.: Teaching and learning virtual strategy for the navigation of multiple-UAV. In: 15th Iberian Conference on Information Systems and Technologies (CISTI) (2020)